JOURNAL OF
POWER
SOURCES

Short communication

# A relation between enhanced Li ion transfer and the improvement in electrochemical performance of a Si–Cu–carbon composite

Yong-Mook Kang [a,*], Min-Sik Park [b], Min-Sang Song [c], Jai-Young Lee [c,d]

[a] *Energy Laboratory, Corporate R&D Center, Samsung SDI Co. Ltd., 428-5 Gongse-dong, Giheung-gu, Yongin-si, Gyeonggi-do, Republic of Korea*
[b] *ISEM, University of Wollongong, Wollongong, 2522 NSW, Australia*
[c] *Department of Materials Science and Engineering, Korea Advanced Institute of Science and Technology,*
*373-1 Guseong-Dong, Yuseong-gu, Daejeon, Republic of Korea*
[d] *Department of Advanced Technology Fusion, Konkuk University, 1 Hwayang-dong, Kwangjin-gu, Seoul 143-701, Republic of Korea*

## Abstract

Si–carbon composite prepared by mechanical milling showed good cyclic capacity retention until the utilization of Si was limited below 32%, whereas the retention of a Si–Cu–carbon composite obtained by two-step mechanical milling was maintained up to 55%. A comparison between the first charge curves of a Si–carbon composite and a Si–Cu–carbon composite at 0.1 C, indicated that the Si–carbon composite underwent a much higher polarization than the Si–Cu–carbon composite, leading to the difference in utilization of Si. Impedance spectroscopy let us confirm that the electrochemical alloying between Si and Li$^+$ is much easier in the Si–Cu–carbon composite than in the Si–carbon composite. The superiority of the Si–Cu–carbon composite in kinetics enabled its electrode to have a more homogeneous Li$^+$ concentration after Li$^+$ insertion. Because this phenomenon means that the Si–Cu–carbon composite has a more homogeneous volume expansion than the Si–carbon composite, the disparity in electrochemical performance between the Si–carbon composite and the Si–Cu–carbon composite was attributed to enhanced Li$^+$ transfer in the Si–Cu–carbon composite.
© 2006 Elsevier B.V. All rights reserved.

*Keywords:* Si–Cu–carbon; Li ion transfer; Li$^+$ depth profile; Volume expansion; Li ion battery

## 1. Introduction

The fast technological progress in the area of portable devices puts higher demands on the portable power supplies. Currently, it seems that the system of choice for high capacity batteries is the Li ion secondary battery, which is typically composed of a carbon negative electrode and a LiCoO$_2$ positive electrode. However, with growing demand for a higher capacity, low capacity of carbon (theoretical capacity: 372 mAh g$^{-1}$) has become a limiting factor in wider applications, and a high capacity alternative to carbonaceous material have thus been sought [1,2]. Among various materials for the negative electrode, some of the most promising materials include Si, Sn and alloys containing these elements [3–5]. Because elements like Sn and Si can alloy and de-alloy with Li$^+$ reversibly and show a low operating

potential when used as the electrode material, they are reasonably adequate as anodes for Li ion secondary batteries. However, they have been reported to suffer an enormous volume expansion during Li$^+$ insertion, which results in poor cyclic properties [4].

Considerable effort has been made to overcome this limitation by using composite materials, in which an electrochemically active phase (Si) is homogeneously dispersed within an electrochemically inactive matrix [6]. The electrochemically inactive phase was mainly a soft and ductile matrix, which can accommodate the mechanical stresses/strains experienced by the active phase. In recent years, several authors have reported that Si/C based composites, prepared using high energy mechanical milling and/or decomposition of organic precursors, show a higher reversible capacity with respect to graphite and better capacity retention with respect to pure silicon [7,8]. However, the application of Si/C based composite materials failed to thoroughly exclude the cyclic degradation that also consists in Si. In Dahn's in situ AFM result, it was clearly observed that during

* Corresponding author. Tel.: +82 16 257 9051; fax: +82 31 288 4504.
*E-mail address:* dake@kaist.ac.kr (Y.-M. Kang).

Li$^+$ insertion into Si based composites, Si particles undergo inhomogeneous volume expansion [9]. This phenomenon means that alloying or de-alloying between Li$^+$ and Si cannot be homogeneously completed in the Si composite materials including Si/C based composites. It was well known that among several steps in the electrochemical reaction, the reaction rate is mainly determined by the charge transfer step around the reaction interface supposing that sufficient ions are supplied for that reaction [10]. Considering this point, it could be expected that the addition of transition metals to the Si/C based materials may be helpful to make Li$^+$ homogeneously alloy or de-alloy with Si because the transition metals are capable of enhancing Li$^+$ transfer by making electronic pathways around the Si particles. So, in this paper, we attempted to prepare a Si–Cu–C composite, which should undergo a more homogeneous volume expansion compared to a Si–C composite.

## 2. Experimental

### 2.1. Preparation of the sample and basic electrochemical measurements

Two-step mechanical milling was used to prepare the Si–Cu–carbon composites. During the first step, a mixture of Si and Cu (80 wt.%:20 wt.%) was mechanically milled using a SPEX-8000 high energy ball-miller. After milling for 4 h, it was confirmed by XRD analysis (Fig. 1) that the mixture of Si and Cu changed into a composite, which was composed of Si, Cu and Cu$_3$Si. In the second step, the mixture of the Si–Cu composite and a crystalline carbon (granular type, $D_{50} = 17 \mu m$) was milled for 30 min to obtain our final material: "Si–Cu–carbon composite". (This short-time milling was applied to avoid destroying the crystallinity of the carbon.) For electrochemical measurements, electrodes were fabricated using a mixture, which was composed of 75 wt.% sample material and 15 wt.% acetylene black. A solution containing 10 wt.% PVDF (poly-vinyledene fluoride) binder in NMP ($n$-methyl-2-pyrrolidinone) was added to this

mixture. Cu mesh was then used for coating this mixture. After the electrode was dried at 110 °C for 2 h in vacuum ($10^{-3}$ Torr), it was compressed under a pressure of about 180 kg cm$^{-2}$. Coin-type cells were used for the charging/discharging experiment, and this experiment was not a full cell test but a half cell test. Assemblies were carried out in an Ar-filled glove box with less than 1 ppm each of oxygen and moisture. Li metal foil was used as the counter electrode and the reference electrode, 1 M LiPF$_6$ in ethylene carbonate and diethyl carbonate (3:7) was used as the electrolyte and Celgard 2400 was used as the separator. The anode performance of the sample material was measured in the range: 0.001–1.5 V (versus Li/Li$^+$) at 0.1 C.

### 2.2. Impedance spectroscopy to investigate the Li$^+$ insertion behavior

In order to analyze the electrochemical impedance response, a Solatron 1255 frequency response analyzer (FRA) was used in conjunction with a Solatron 1286 electrochemical interface. After the electrode reached an equilibrium potential, the electrochemical impedance measurements were carried out by applying an ac voltage of 5 mV over the frequency range from 1 mHz to 100 kHz. Nyquist plots during the first charge (Li$^+$ insertion) were closely observed to figure out the difference in the Li$^+$ insertion behavior between the Si–carbon composite and the Si–Cu–carbon composite.

### 2.3. After-cycle analyses (SIMS and SEM)

Examination of the after-cycle electrode involved first disassembling the cell in the glove box, rinsing the electrode twice with dimethyl carbonate and removing the solvent under vacuum. In order to survey the after-first-charge Li$^+$ distribution in the electrode, each electrode containing Si–carbon composite or Si–Cu–carbon composite, was examined by secondary ion mass spectroscopy (SIMS). Then, O$_2^+$ was used as an ion beam source and the current of ion beam was $4 \times 10^{-7}$ A. After 100 cycles, the morphology of the electrodes was confirmed by scanning electro microscopy (SEM) analysis.

## 3. Results and discussion

### 3.1. Electrochemical differences between the Si–carbon composite and Si–Cu–carbon composites

The Si–Cu–carbon composite was prepared by two-step mechanical milling. As a result, it was possible to make this material have a core-shell structure such that the Si–Cu composite was located in the core coated with carbon particles. Close observation of the core part has shown that Cu is homogeneously dispersed in the Si matrix. As mentioned in the experimental section, the Si–Cu–carbon composite was characterized as a mixture of Si, Cu, Cu$_3$Si and carbon (Fig. 1). The cyclic retention of the Si–Cu–carbon composite at different utilizations was compared with that of the Si–carbon composite. The results of the comparison are shown in Fig. 2a. Even if the Si–carbon composite attained a big leap from pure Si in cyclic retention, there
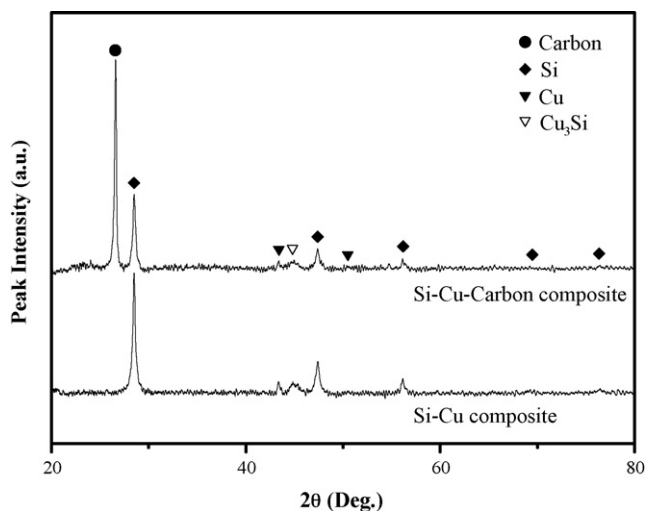


Fig. 1. XRD patterns of Si–Cu composite prepared by mechanical milling for 4 h and Si–Cu–carbon composite by additional milling with carbon for 30 min.
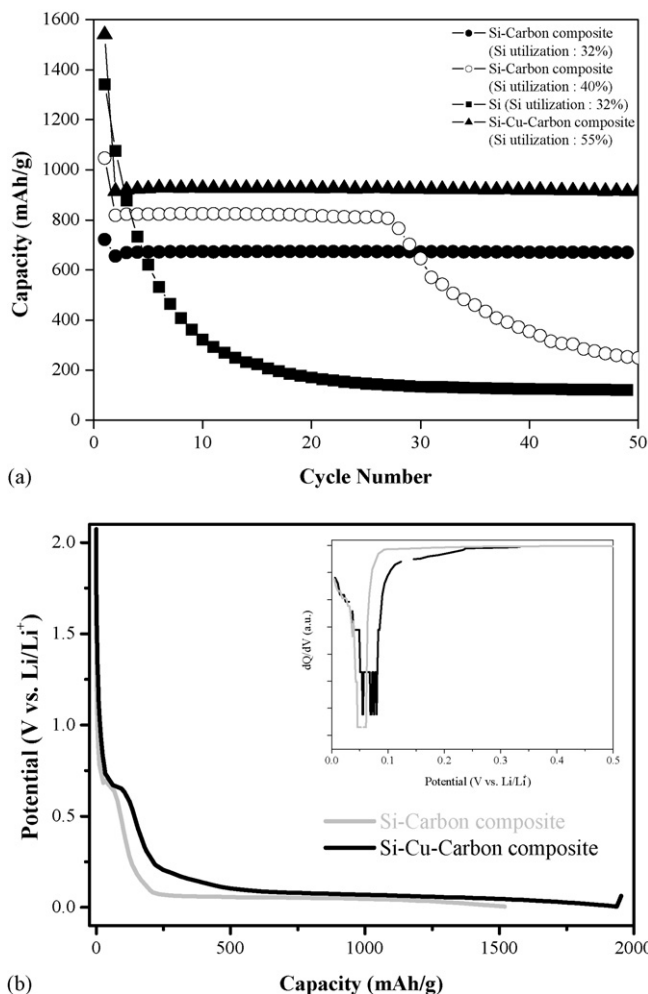
Fig. 2. (a) Cyclic retentions of Si, Si–carbon composite and Si–Cu–carbon composite. (b) A comparison between Si–carbon composite and Si–Cu–carbon composite in first charge (Li$^+$ insertion) behavior; in-box shows d$Q$/d$V$ curves for first charge curves.

was still an inevitable degradation when more than 32% of the Si reacted with Li$^+$. With the utilization of Si below 100% in the Si–carbon composite, some of the utilized parts at every cycle lose electronic contact. Therefore, after it reaches the critical cycle number, Si–carbon composite seems to undergo an abrupt electrochemical degradation. This means that the endurance of the Si–carbon composite against its cyclic degradation was limited to 32% of Si utilization. On the other hand, it is shown by Fig. 2a that Si–Cu–carbon composite exhibited excellent cyclic retention (After 50 cycles, more than 98% of the initial capacity was maintained.) even until Si utilization got to 55%. Hence, if it is commercialized as a novel anode material with high capacity, the capacity of the Si–carbon composite should be limited to 680 mAh g$^{-1}$, whereas the application of a Si–Cu–carbon composite could enhance the capacity of the anode to up to 920 mAh g$^{-1}$. These results imply that we could almost reach 3000 mAh for a 18,650 cylindrical cell.

Fig. 2b shows the first charge curves of the Si–Cu–carbon composite and Si–carbon composite, which were obtained from 0.001 to 1.5 V (versus Li/Li$^+$). By differentiating the charge quantity on the basis of potential in their charge–discharge

curves, it is known that there is no difference in redox reaction. In Fig. 2b, a little hump at the beginning of charge can result from some irreversible reactions that include not only the routine electrolyte decomposition but also Li$^+$ absorption by pores around carbon. Considering that Li$^+$ intercalation between the graphene layers of carbon scarcely occurs in the Si–carbon composites prepared by mechanical milling, it could be thought that the only reversible reaction of Si–Cu–carbon and Si–carbon composites is alloying of Li$^+$ with Si [11]. Because about 250 mAh g$^{-1}$ was involved by irreversible reactions, a comparison between the first charge capacities of Si–Cu–carbon composite (1952 mAh g$^{-1}$) and Si–carbon composite (1284 mAh g$^{-1}$) shows that 99.5% of Si portion was reacted in the Si–Cu–carbon composite, whereas only 61% was available in the Si–carbon composite. Based on the observation that closed circuit voltage (CCV) of the Si–Cu–carbon composite in the charging plateau, which is developed by the amorphization of Si during Li$^+$ insertion, is much higher than that of Si–carbon composite, it could be said that the former undergoes much less polarization than the latter. This result shows that Li$^+$ insertion into Si–Cu–carbon composite may be much easier than that into the Si–carbon composite. In order to confirm this hypothesis, EIS analyses were conducted for Si–Cu–carbon and Si–carbon composites at 1, 0.5, 0.05 and 0.01 V (versus Li/Li$^+$) during first charge (Fig. 3). Fig. 3 shows that during Li$^+$ insertion into these materials, there were two semicircles related to two kinds of resistance. The first semicircle at higher frequency is correlated with the formation of a passivation film on the surface and the second semicircle at lower frequency is related to the Li$^+$ charge transfer at the interface. As observed in carbonaceous material, Li$^+$ insertion tends to make the charge transfer resistance apparently restrained. Because alloying between Li$^+$ and Si involves the augmentation of surface area, which is in inverse proportion to the resistance as indicated by "$R = \rho$ (resistivity) $L$ (length)/$A$ (surface area)", Li$^+$ insertion into Si based material can make the reduction of charge transfer resistance more prominent [10]. So, it could be thought that the reduction of charge transfer resistance is a measure to indicate which, between Si–Cu–carbon composite and Si–carbon composite, is more susceptible to Li$^+$ transfer. Based on this fact, a comparison between the charge transfer resistances of Si–Cu–carbon composite and Si–carbon composite at several potentials during first charge shows that the electrochemical insertion of Li$^+$ is much easier in Si–Cu–carbon composite than in Si–carbon composite (Fig. 3). Therefore, it could be expected that there is a disparity between the Si–Cu–carbon composite and Si–carbon composite in the susceptibility to Li$^+$ transfer.

### 3.2. Relation between volume expansion and Li$^+$ distribution in the electrode

Fig. 4 presents the Li$^+$ depth profiles in the electrodes each containing Si–Cu–carbon composite and Si–carbon composite. To compare the Li$^+$ distribution in the Si–Cu–carbon composite with that in the Si–carbon composite, secondary ion mass spectroscopy (SIMS) analysis was carried out using O$_2^+$ as the ion source. When Li$^+$ was inserted up to 0.001 V versus Li/Li$^+$
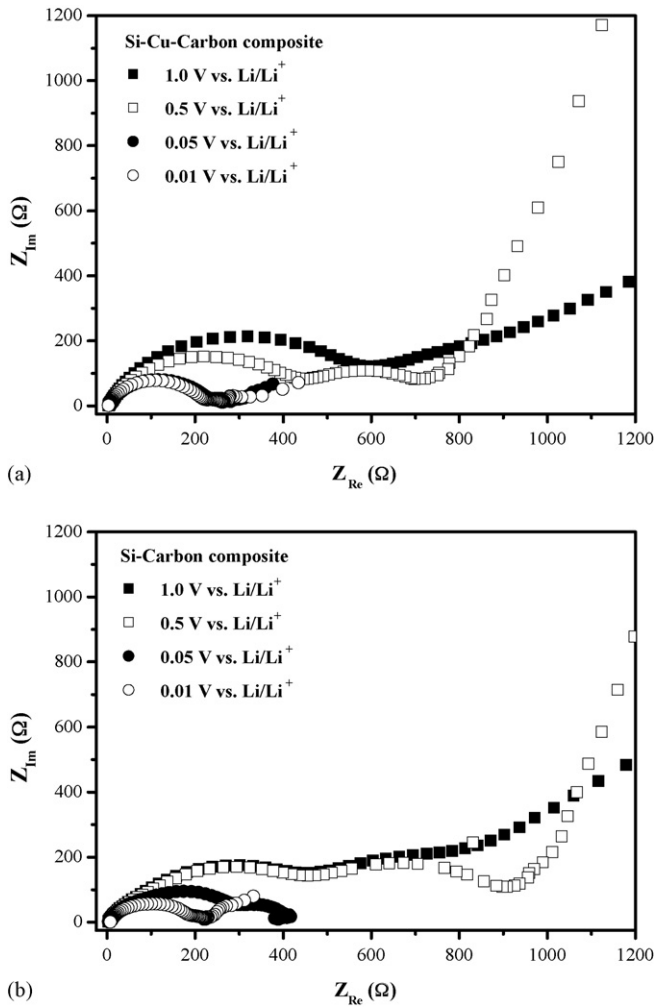
Fig. 3. Nyquist plots of: (a) Si–Cu–carbon composite and (b) Si–carbon composite obtained at 1, 0.5, 0.05, 0.01 V (vs. Li/Li$^+$) during first charge (Li$^+$ insertion).

at 0.1 C, the electrode composed of Si–Cu–carbon composite exhibited a very homogeneous depth profile for Li$^+$, while the electrode composed of Si–carbon composite had a clear disparity in Li$^+$ concentration between shallow depth and deep depth.
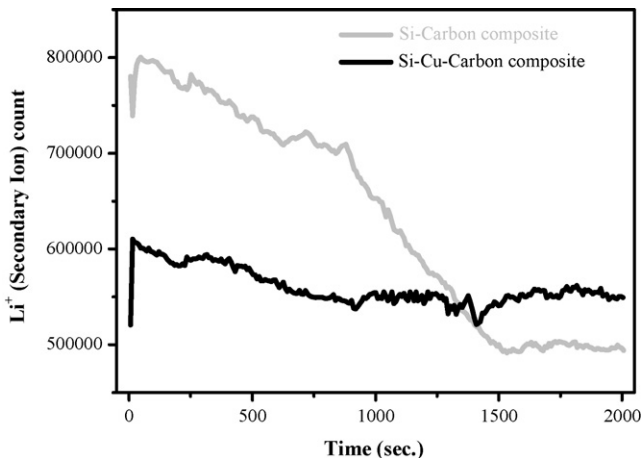


Fig. 4. Li$^+$ distribution (from SIMS analysis) in Si–Cu–carbon composite and Si–carbon composite after first charge (Li$^+$ insertion).

As mentioned in the previous paragraph, this phenomenon is because Si–Cu–carbon composite is more susceptible to Li$^+$ transfer than Si–carbon composite. It seems that the enhanced Li$^+$ transfer in the Si–Cu–carbon composite enabled its electrode to have a more homogeneous Li$^+$ concentration after Li$^+$ insertion. When attempting to clarify the reason for the difference of susceptibility to Li$^+$ transfer, two factors such as electronic pathways enhanced by Cu particles and more incorporated pores can be considered. Barret–Joiner–Halenda (BJH) analysis indicated that the Si–Cu–carbon composite has the same number of pores as the Si–carbon composite. Furthermore, SEM electron mapping for Si–Cu–carbon composite showed that Cu particles were uniformly distributed around the Si particles. Hence, it is known that Cu particles play a crucial role in the enhanced susceptibility to Li$^+$ transfer in Si–Cu–carbon composite. (Further work is underway to identify the detailed reason for the enhancement of Li$^+$ transfer in Si–Cu–carbon composite.)

Fig. 5 demonstrates the effect of the homogeneity of Li$^+$ distribution on the morphological change of electrode. As shown in this figure, the electrode containing Si–Cu–carbon composite had some minor cracks without severe pulverization even after 50 cycles. On the other hand, large pulverization (induced by crumbling of Si particles) was observed in the electrode comprised of Si–carbon composite. In conjunction with SIMS results (Fig. 4), it could be said that an homogeneous reaction between Li$^+$ and Si parts in Si–Cu–carbon composite helps to exclude a
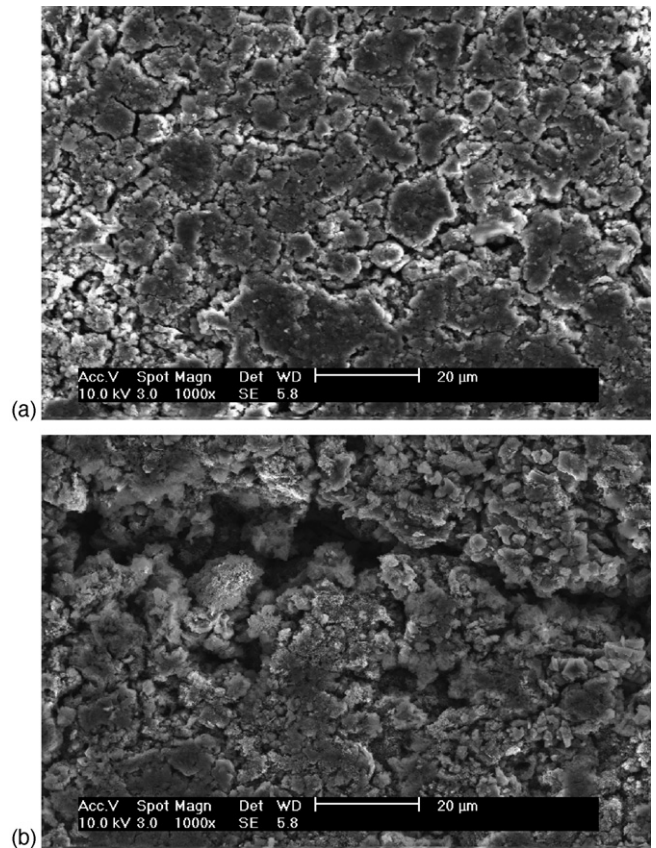




Fig. 5. Morphological difference between the electrodes each including (a) Si–Cu–carbon composite and (b) Si–carbon composite after 50 cycles (50 times repetition of alloying or de-alloying between Li$^+$ and Si).

partial concentration of volume expansion, which was evolved by a supersaturated reaction between Li$^+$ and some of Si parts in Si–carbon composite [12].

## 4. Conclusions

In conclusion, the results reported here show that with the help of Cu particles uniformly dispersed around Si, the cyclic retention of a Si–Cu–carbon composite is greatly improved compared to a Si–carbon composite. Some electrochemical results such as Nyquist plots from EIS analysis and charge/discharge curves obtained at 0.1 C suggest that in the susceptibility to Li$^+$ transfer, there is a clear disparity between the Si–Cu–carbon and Si–carbon composites. This can be explained by enhanced Li$^+$ transfer in the Si–Cu–carbon composite so that the Si–Cu–carbon composite has a more homogeneous Li$^+$ distribution than the Si–carbon composite. This result enables us to suggest that a Si–Cu–carbon composite undergoes a more homogeneous volume expansion than a Si–carbon composite as shown in the after-cycle morphology of their electrodes. Finally, we believe that these results provide important evidence that the improved electrochemical performance of a Si–Cu–carbon composite is due to the enhanced Li$^+$ transfer.

## References

[1] J.R. Dahn, A.K. Sleigh, H. Shi, J.N. Reimers, O. Zhong, B.M. Way, Electrochim. Acta 38 (1993) 1179.
[2] R. Yazami, D. Guerard, J. Power Sources 43/44 (1993) 39.
[3] Y. Idota, T. Kubota, A. Matsufuji, Y. Maekawa, T. Miyasaka, Science 276 (1997) 1395.
[4] I.A. Courtney, J.S. Tse, O. Mao, J. Hafner, J.R. Dahn, Phys. Rev. B 58 (1999) 15583.
[5] M. Winter, J.O. Bessenhard, Electrochim. Acta 45 (1999) 31.
[6] I.S. Kim, P.N. Kumta, G.E. Blomgren, Electrochem. Solid State Lett. 3 (2000) 493.
[7] D. Larcher, C. Mudalige, A.E. George, V. Porter, M. Gharghouri, J.R. Dahn, J. Power Sources 122 (1999) 71.
[8] K.J. Gross, J.C.F. Wang, G.A. Roberts, US. Patent US2004/137,327 A1 (2004).
[9] L.Y. Beaulieu, K.W. Eberman, R.L. Turner, L.J. Krause, J.R. Dahn, Electrochem. Solid State Lett. 4 (2001) A137.
[10] J.R. Macdonald, Impedance Spectroscopy, Wiley, 1987.
[11] N. Dimov, S. Kugino, M. Yoshio, J. Power Sources 136 (2004) 108.
[12] A. Timmons, J.R. Dahn, J. Electrochem. Soc. 153 (2006) A1206.